On the Acceleration of Free Fall inside Polyhedral Structures

Hartmut Müller, Renata Angeli, Roberta Baccara, Flavia Contenti, Rose Line Hofmann, Simona Muratori, Giuliana Papa, Francesca Santoni, Alessandro Turiano, Simona Turiano, Claudio Venegoni, Leili Khosravi

E-mail: hm@interscalar.com

In this paper we develop a fractal model of matter as stable eigenstates in chain systems of harmonic quantum oscillators and derive a fractal scalar field that should affect any type of physical interaction, regardless of its complexity. Based on this assumption, we discuss series of experiments on the timing of free falling solid particles inside polyhedral structures whose boundaries coincide with equipotential surfaces of the field.

Introduction

An essential aspect of scientific research is the distinction between empirical facts and theoretical models. This is not only about honesty and ethics in science, but a crucial condition of its evolution. The scientist should always be aware of this.

The nature and origin of gravitation is a key topic in modern physics. Gravitation manifests itself as universal force of attraction. It decreases with increasing distance, but it is thought as having unlimited range. Unlike electrical or magnetic forces, gravitation is considered as to be not shieldable.

The term 'gravitational shielding' is usually imagined as effect of reducing the weight of an object located in a constant gravitational field, neither changing the mass of the object nor its location in that field. Gravitational shielding is considered to be a violation of the equivalence principle and therefore inconsistent with both Newtonian theory and general relativity.

Nevertheless, some experimental evidence [1] indicates that such effect might exist under quite exotic conditions in which a superconductor is subjected to peak currents in excess of 10^4 A, surface potentials of 10^6 V, magnetic fields up to 1 T, and temperature down to 40 K.

In the context of classical physics, mass is considered as source of gravitation described by the Newtonian 'law of universal gravitation' as an instantaneous force acting through empty space. A fundamentally different understanding of gravitation arises from Einstein's general theory of relativity. In this case, gravity acts through a hypothetical 'curvature of space-time', while any kind of energy can cause it.

Gravitation is treated as dominant force at macroscopic scales that forms the shape and trajectory (orbit) of astronomical bodies including stars and galaxies. Advanced models were developed [2–4] in the last century which explain essential features of the formation of the solar system. Though, if numerous bodies are gravitationally bound to one another, classic models predict long-term highly unstable states that contradict with the astrophysical reality in the solar system.

Furthermore, many metric characteristics of the solar system are not predicted in standard models. A remarkably large number of coincidences are considered to be accidental and are not even topics of theoretical research. Until today none of the standard models of gravitation could explain why the solar system has established Jupiter's orbital period at 11.86 years and not 10.27 or 14.69 years; why the Sun and the Moon, the gas giant Jupiter and the planetoid Ceres, but also Earth and Mars have similar rotation periods; why Venus and Uranus, as well as Mars and Mercury have similar surface gravity accelerations; why several exoplanets in the Trappist 1 system have the same orbital periods as the moons of Jupiter, Saturn and Uranus etc. etc.

The standard theory of gravitation experiences also exceptional difficulties to explain the dynamics in star systems. The orbital velocities of stars should decrease in an inverse square root relationship with the distance from the Galactic Center, similar to the orbital velocities of planets in the solar system. But this is not observed. Outside of the central galactic bulge the orbital velocities are nearly constant.

Already in 1933, Fritz Zwicky [5] discovered that the fast movement of the galaxies in the Coma Cluster cannot be explained by the gravity effect of the visible galaxies only and hypothesized the existence of unseen mass that he called 'dark matter'. In 1957, Henk van de Hulst and then in 1959, Louise Volders demonstrated that the galaxies M31 and M33 do not spin as expected in accordance with Kepler's laws.

According to the hypothesis of mass as source of gravity, this deviation might be explained by the existence of a substantial amount of matter flooding the galaxy that is not emitting light and interacts barely with ordinary matter and therefore it is not observed. To explain the dynamics in galaxies and clusters, standard theories of gravitation need a lot of dark matter - 85% of the matter in the universe. Even particle physics has no idea what dark matter could be.

Nevertheless, it is still believed that gravitation of mass determines the orbits of planets and moons, planetoids and asteroids, comets and artificial satellites, and in the cosmos, the formation of stars and galaxies and their evolution. It is also thought that it is the mass of the Earth that causes all bodies to fall 'down'.

The universality of free fall means that the gravity acceleration of a test body at a given location does not depend on its mass, form, physical state or chemical composition. This

discovery, made four centuries ago by Galilei, is confirmed by modern empirical research with an accuracy of $10^{-11} - 10^{-12}$. A century ago Einstein supposed that gravity is indistinguishable from, and in fact the same thing as, acceleration. Indeed, Earth's surface gravity acceleration can be derived from the orbital elements of any satellite, also from Moon's orbit:

$$g = \frac{\mu}{r^2} = \frac{\mu}{(6372000\ \mathrm{m})^2} = 9.82\ \mathrm{m/s^2}$$

$$\mu = 4\pi\frac{R^3}{T^2} = 3.9860044 \cdot 10^{14}\ \mathrm{m^3/s^2}$$

where R is the semi-major axis of Moon's orbit, T is the orbital period of the Moon and r is the average radius of the Earth. No data about the mass or chemical composition of the Earth or the Moon is needed.

The 3^{rd} law of Johannes Kepler describes the ratio R^3/T^2 as constant for a given orbital system. Kepler's discovery is confirmed by high accuracy radar and laser ranging of the movement of artificial satellites.

Actually, Kepler's 3^{rd} law is of geometric origin and can be derived from Gauss's flux theorem in 3D-space within basic scale considerations. It applies to all conservative fields which decrease with the square of the distance and does not require the presence of mass.

It is important to underline that the orbital elements R and T are measured, but $\mu = GM$ is a theoretical presumption that provides mass as a source of gravity and the universality of the coefficient G, the 'gravitational constant'.

One of the basic principles of scientific research is the falsifiability of a theory. Occam's Razor that expresses the preference for simplicity in the scientific method is mainly based on the falsifiability criterion: simpler theories are more testable.

Obviously, any theory that postulates gravitation of mass as dominant forming factor of the solar system and the galaxy is not falsifiable, because there is no independent method to measure the mass of a celestial body. Actually, no mass of any celestial body is measured, but only calculated based on the theoretical presumption $\mu = GM$, and G is estimated in laboratory scale only.

This does not mean that those theories are compellingly wrong, but it should not surprise anyone if the assumption G = constant leads to problems in describing processes that differ by 40 orders of magnitude.

The big G is known only to three decimals, because gravity appears too weak on the scale of laboratory-sized masses for to be measurable with higher precision. As mentioned Quinn and Speake [6], the discrepant results may demonstrate that we do not understand the metrology of measuring weak forces or they may signify some new physics.

In the case of mass as source of gravity, in accordance with Newton's shell theorem, a solid body with a spherically symmetric mass distribution should attract particles outside it as if its total mass were concentrated at its center. In contrast, the attraction exerted on a particle should decrease as the particle goes deeper into the body and it should become zero at the body's center.

The Preliminary Reference Earth Model [7] affirms the decrease of the gravity acceleration with the depth. However, this hypothesis is still under discussion. In 1981, Stacey, Tuck, Holding, Maher and Morris [8, 9] reported anomalous measures (larger values than expected) of the gravity acceleration in deep mines and boreholes. In [10] Frank Stacey writes: "Modern geophysical measurements indicate a 1% difference between values at 10 cm and 1 km (depth). If confirmed, this observation will open up a new range of physics".

Anomalies have been discovered also under conditions of microgravity – in drop towers, abroad the NASA Space Shuttle and the ISS. Whenever an object is in free fall the condition of microgravity comes about. Microgravity significantly alters many processes – the behavior of liquids [11], plasma and granular materials [12, 13] as well, and there is no complete explanation for all the discovered phenomena yet.

Studies [14] of plant growth under different gravity conditions show that elongation growth is stimulated under microgravity conditions. Elongation growth is suppressed with increasing gravitational acceleration and varies in proportion to the logarithm of the magnitude of gravitational acceleration in the range from microgravity to hypergravity.

Already in 2010, Erik Verlinde [15] proposed an alternative explanation of gravitation as an entropic force caused by changes in the information associated with the positions of material bodies. An entropic force is thought as an effective macroscopic force that originates in a system with many degrees of freedom by the statistical tendency to increase its entropy. The term 'entropic force' was introduced by Bechinger and Grünberg [16] when they did demonstrate that in systems of particles of different sizes, entropy differences can cause forces of attraction between the largest particles. However, entropic models of gravitation [17] are still in development and under discussion [18].

It is remarkable that similar dynamics of plant growth observed in laboratory [19] and field experiments [20] are also known as the 'pyramid effect': Inside pyramidal constructions made of various materials, germination and elongation growth of plants are accelerated.

The diversity of sizes and materials (glass, plastic, wood, stone, metal) applied in the pyramidal constructions makes difficult to define the cause of the observed growth stimulation. At the same time, even this diversity supports the suspicion that the 'pyramid effect' could be caused by reduction of gravitation – as it is the most universal physical interaction.

To verify this hypothesis, we have designed an experimental setup that models the free fall of solid particles inside containers of various sizes, shapes and materials. The experimental design is based on global scaling [21] and considers Kosyrev's [22] temporal studies.

Methods

In [23] we have introduced a fractal model of matter as stable eigenstates in chain systems of harmonic quantum oscillators and could show the evidence of this model for all known hadrons, mesons, leptons and bosons as well. On this background, atoms and molecules emerge as eigenstates of stability in fractal chain systems of harmonically oscillating protons and electrons. Andreas Ries [24] demonstrated that this model allows for the prediction of the most abundant isotope of a given chemical element.

In [25] we have shown that the set of stable eigenstates in chain systems of harmonic quantum oscillators is fractal and can be described by finite continued fractions:

$$\mathcal{F}_{jk} = \ln(\omega_{jk}/\omega_{00}) = [n_{j0}; n_{j1}, n_{j2}, \ldots, n_{jk}]$$

where ω_{jk} is the set of angular eigenfrequencies and ω_{00} is the fundamental frequency of the set. The denominators are integer: $n_{j0}, n_{j1}, n_{j2}, \ldots, n_{jk} \in \mathrm{Z}$, the cardinality $j \in \mathrm{N}$ of the set and the number $k \in \mathrm{N}$ of layers are finite. In the canonical form, all numerators equal 1.

Any finite continued fraction represents a rational number [26]. Therefore, the ratios ω_{jk}/ω_{00} of eigenfrequencies are always irrational, because for rational exponents the natural exponential function is transcendental [27].

This circumstance provides for lasting stability of those eigenstates of a chain system of harmonic oscillators because it prevents resonance interaction [28, 29] between the elements of the system. In [30, 31] we have applied our model as criterion of stability in engineering.

The distribution density of stable eigenstates reaches local maxima near reciprocal integers $\pm 1/2, \pm 1/3, \pm 1/4, \ldots$ that are the subattractor points in the fractal set $\mathcal{F}_{jk}$ of natural logarithms (fig. 1). Integer logarithms $0, \pm 1, \pm 2, \ldots$ represent the most stable eigenstates (main attractors).

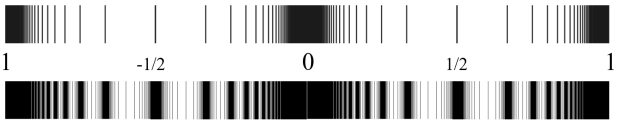

Fig. 1: The distribution of stable eigenvalues of $\mathcal{F}_{jk}$ for $k = 1$ (above) and for $k = 2$ (below) in the range $-1 \leqslant \mathcal{F}_{jk} \leqslant 1$.

In the case of harmonic quantum oscillators, the continued fractions $\mathcal{F}_{jk}$ define not only fractal sets of natural angular frequencies ω_{jk}, angular accelerations $a_{jk} = c \cdot \omega_{jk}$, oscillation periods $\tau_{jk} = 1/\omega_{jk}$ and wavelengths $\lambda_{jk} = c/\omega_{jk}$ of the chain system, but also fractal sets of energies $\mathrm{E}_{jk} = \hbar \cdot \omega_{jk}$ and masses $\mathrm{m}_{jk} = \mathrm{E}_{jk}/c^2$ which correspond with the eigenstates of the system. For this reason, we call the continued fraction $\mathcal{F}_{jk}$ the 'Fundamental Fractal' of stable eigenstates in chain systems of harmonic quantum oscillators.

The spatio-temporal projection of the Fundamental Fractal $\mathcal{F}_{jk}$ of stable eigenstates is a fractal scalar field of transcendental attractors, the Fundamental Field.

The connection between the spatial and temporal projections of the Fundamental Fractal is given by the speed of light $c = 299792458$ m/s. The constancy of c makes both projections isomorphic, so that there is no arithmetic or geometric difference. Only the units of measurement are different.

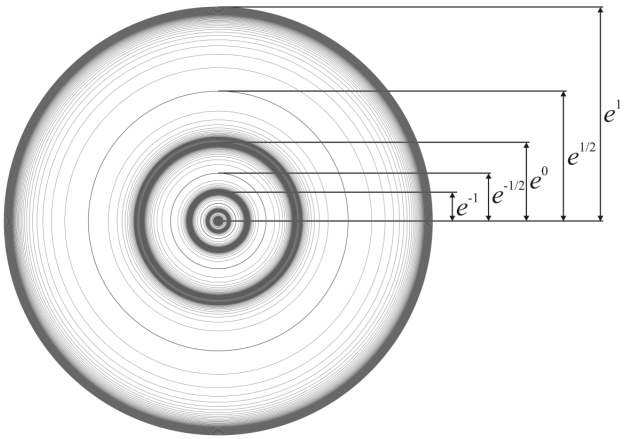

Fig. 2: The equipotential surfaces of the Fundamental Field in the linear 2D-projection for $k = 1$.

Figure 2 shows the linear 2D-projection $\exp(\mathcal{F}_{jk})$ of the first layer of the Fundamental Field for $\mathcal{F}_{j1} = n_{j0} + 1/n_{j1}$ in the interval $-1 < \mathcal{F}_{j1} < 1$. Figure 1 shows the same interval in the logarithmic representation.

At each layer k, the potential energy of the Fundamental Field is constant, therefore the layers are equipotential surfaces. The potential difference defines a gradient, a vector directed to the center of the field that causes a central force of attraction. However, the gradient exposes the logarithmically hyperbolic fractal metric of the Fundamental Field.

The Fundamental Field does not propagate, it is omnipresent. As spatio-temporal projection of the Fundamental Fractal, it is an inherent feature of the number continuum and it causes the fractality of the model space-time.

In physics, only field distortions (waves or currents), not the fields themselves have propagation speeds. In astronomic calculations, gravitation is traditionally considered as being instantaneous. First Laplace [32] demonstrated that gravitation as field does not propagate with the speed of light c. Modern estimations [33] confirm a lower limit of $2 \cdot 10^{10}\, c$.

The Fundamental Field is of pure mathematical origin, and there is no particular physical mechanism required as field source. It is all about numbers as ratios of physical quantities which inhibit destabilizing resonance. In this way, the Fundamental Field concerns all repetitive processes which share at least one characteristic — the frequency.

Therefore, we assume the universality and unity of the Fundamental Field. It might signify that everything in the universe is part of one giant oscillating chain system. This hypothesis we have called 'global scaling' and it is the basis of interscalar cosmology [34].

In fact, scale relations in particle physics [23, 35, 36] and nuclear physics [24, 37, 38], astrophysics [39, 40] and biophysics [41,42] follow always the same Fundamental Fractal calibrated on the proton and electron, without any additional or particular settings. The proton-to-electron mass ratio itself is caused by the Fundamental Fractal [34].

Planetary and lunar orbits [43] correspond with equipotential surfaces of the Fundamental Field, as well as the metric characteristics of stratification layers in planetary atmospheres [44] and lithospheres [21]. Surface gravity accelerations [45] of the planets in the solar system correspond with attractors of stability in chain systems of oscillating protons and electrons. From this point of view, the metric characteristics of stable structures origin always from the same Fundamental Fractal and different only in scale. Because of its numerical origin, we assume that the Fundamental Field affects any type of physical interaction, regardless of its complexity.

Based on this assumption, we have designed an experimental setup that models the free fall of solid particles inside a container whose boundaries coincide with equipotential surfaces of the Fundamental Field $\exp(\mathcal{F}_{jk})$. The experimental setup consists of a vacuum hourglass (sand clock) and a closed container. The duration of the hourglass was measured inside and outside the container in alternating sequence.

Three different in size, material and duration (40 s, 8 min, 60 min) hourglasses and 18 different in shape (cubic, tetrahedral, octahedral), size (0.3 – 0.6 m diameter) and material (carton, acrylic glass, metal) containers were used.

Based on relevant studies [46], we conducted mechanical tests of the utilized hourglasses and could make sure that inclination below 5 degrees, rotation below 5 Hz and microvibration (vertical and horizontal) below 10 Hz do not increase the average fluctuation level (0.2 %) of the duration of the hourglasses.

The accuracy of the vertical was controlled by two orthogonal spirit levels. The complete setup was placed in an electromagnetic shielding chamber. During the measurement, the hourglass had direct contact to an aluminum plate for conduction of eventual electrostatic charge.

The environment control included electromagnetic fields in the frequency range of 1 Hz to 5 GHz, air temperature, pressure and humidity, micro-seismic activity. The experiments were conducted in different places, but always far from the city electrification net.

Results

In general, the measured deviations of the hourglass durations inside containers of different material, shape and size in comparison with the durations outside them did not exceed the average fluctuation level of the duration of the used hourglass. However, a stable significant deviation in the hourglass duration was measured with the 8-minute vacuum hourglass inside a closed truncated octahedron (fig. 3) made of 1/16 aluminum sheet. The 'sand' of this hourglass consists of glass beads of ca. 50 μm diameter.

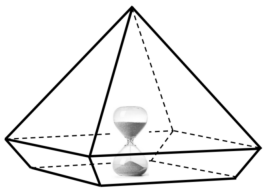

Fig. 3: The duration of the 8-minute hourglass was measured inside and outside the truncated octahedron in alternating sequence.

The truncated octahedron one can imagine as a square pyramid plus an inversed square frustum (fig. 3). The length of the edges of the pyramid coincides with the radius of the main equipotential surface $\mathcal{F}(35)$ of proton stability:

$$\mathcal{F}(35) = \lambda_{\text{proton}} \cdot \exp(35) = 33 \text{ cm}$$

Considering the height $r = 33 \text{ cm} \cdot \sqrt{2}/2 = 23$ cm of the pyramid, the orifice of the hourglass was placed in a distance from the vertices of the pyramid that equals to the radius of the main equipotential surface $\mathcal{F}(27)$ of electron stability:

$$\mathcal{F}(27) = \lambda_{\text{electron}} \cdot \exp(27) = 21 \text{ cm}$$

The height 7.5 cm of the frustum coincides with the radius of the main equipotential surface $\mathcal{F}(26)$ of electron stability:

$$\mathcal{F}(26) = \lambda_{\text{electron}} \cdot \exp(26) = 7.5 \text{ cm}$$

Furthermore, at 6 minutes after start, the continuing process of free fall passes the main temporal attractor $\mathcal{F}(54)$ of electron stability:

$$\mathcal{F}(54) = \tau_{\text{electron}} \cdot \exp(54) = 6 \text{ min}$$

The Compton angular wavelength of the electron is $\lambda_{\text{electron}} = 3.86159\dot{1}0^{-13}$ m, of the proton $\lambda_{\text{proton}} = 2,10308\dot{1}0^{-16}$ m, and the angular oscillation period of the electron is $\tau_{\text{electron}} = \lambda_{\text{electron}}/c = 1.28808\dot{1}0^{-21}$ s [47].

Probably, all these coincidences together caused an accumulated effect of damping the acceleration of free fall. Furthermore, we suppose that potential differences between equipotential surfaces of the Fundamental Field can change the entropy of the involved processes.

In series of crystallization experiments, we observed that inside the same truncated octahedron, sodium chloride crystals grow in salt solutions with concentrations far below the saturated concentration and develop octahedral shapes like diamonds instead of cubic.

The most widely accepted law that predicts the flowrate of mono-sized grains through an orifice and its dependence on different parameters was proposed by Beverloo, Leniger and van de Velde [48, 49]. They have shown that under otherwise

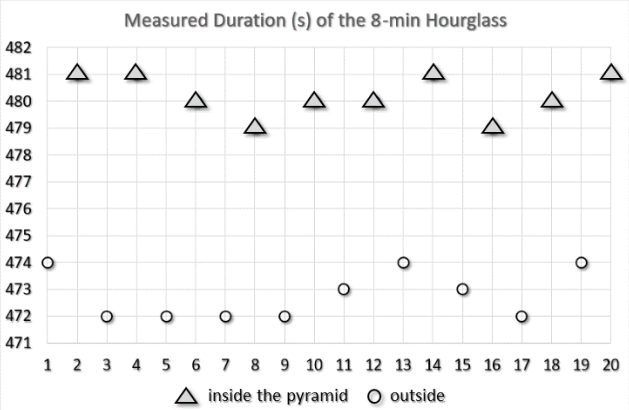

Fig. 4: Time series of the alternating measurements of the hourglass duration (s) inside the truncated octahedron (pyramid) and outside.

constant conditions k, the mass flowrate W is proportional to the square root of the gravity acceleration g:

$$W = k\sqrt{g}$$

This equation coincides with Torricelli's law for the speed of fluid flowing out of an orifice and allows for estimation of the equivalent gravity reduction Δg that corresponds to the ratio of the measured durations inside and outside the octahedron:

$$\Delta g = g\left(\frac{t_{\text{outside}}}{t_{\text{inside}}}\right)^2 - g$$

Table 1 contains representative samples of the durations measured inside and outside the truncated octahedron and the calculated corresponding equivalent gravity reduction in units of g. Fig. 1 shows time series of the alternating measurements.

series	out, s	inside, s	inside/out-1, %	Δg
1	474	481	1.48	-0.283
2	472	481	1.91	-0.364
3	472	480	1.69	-0.324
4	472	479	1.48	-0.285
5	472	480	1.69	-0.324
6	473	480	1.48	-0.284
7	474	481	1.48	-0.283
8	473	479	1.27	-0.244
9	472	480	1.69	-0.324
10	474	481	1.48	-0.283
average	473 ± 1	480 ± 1	1.57	-0.300

Table 1: The measured duration (s) of the 8-minute hourglass inside the truncated octahedron and outside, the relative deviation and the equivalent gravity reduction in units of g.

Over all series of the total 255 hours of measurements, the fluctuation level of the hourglass durations inside and outside the truncated octahedron did not exceed 0.2 %. The relative difference of the durations inside and outside the octahedron did not fall below 1.2%. The average relative difference was 1.67% that corresponds to an equivalent gravity reduction of -0.324 g inside the octahedron. Outside the octahedron, this amount of gravity reduction would correspond to an altitude of 100 km over sea level.

Only inside the described truncated octahedral container we observed a stable significant deviation in the duration of the hourglass, regardless of the location and time. In containers of different shape and size, even made of the same 1/16 aluminum sheet, the measured deviations did not exceed the average fluctuation level of the hourglass duration.

Currently we have no explanation for the extraordinariness of the octahedral (pyramidal) shape. However, in Finslerian multi-dimensional time models, the pseudo-Euclidean light cone becomes a light pyramid [50].

Conclusion

We are aware that our experiments cannot claim to be conclusive. However, they could point out that gravity is not just about the amount of the involved masses and energies. It may well be that 'subtle' factors like the spatial configuration of the system and its scale have higher influence than expected.

Acknowledgements

The authors are grateful to the Community of Living Ethics for permanent support on all stages of the study.

Submitted on September 20, 2018

References

1. Podkletnov E., Modanese G. Impulse Gravity Generator Based on Charged $YBa_2Cu_3O_{7-y}$ Superconductor with Composite Crystal Structure. arXiv:physics/0108005v2 [physics.gen-ph], (2001).
2. Williams I.O., Cremin A.W. A survey of theories relating to the origin of the solar system. *Qtly. Rev. RAS*, 1968, v. 9, 40–62.
3. Van Flandern T. Our Original Solar System – a 21st Century Perspective. *MetaRes. Bull.*, 2008, v. 17, 2–26.
4. Woolfson M.M. Planet formation and the evolution of the Solar System. arXiv:1709.07294, (2017).
5. Zwicky F. On the Masses of Nebulae and of Clusters of Nebulae. *The Astrophysical Journal*, 1937, v. 86, 217.
6. Quinn T., Speake C. The Newtonian constant of gravitation – a constant too difficult to measure? An introduction. *Phil. Trans. Royal Society A*, 2014, v. 372, 20140253.
7. Dziewonski A.M., Anderson D.L. Preliminary reference Earth model. *Physics of the Earth and Planetary Interiors*, 1981, v. 25, 297–356.
8. Stacey F.D. et al. Constraint on the planetary scale value of the Newtonian gravitational constant from the gravity profile within a mine. *Phys. Rev. D*, 1981, v. 23, 1683.
9. Holding S.C., Stacey F.D., Tuck G.J. Gravity in mines. An investigation of Newton's law. *Phys. Rev. D*, 1986, v. 33, 3487.
10. Stacey F.D. Gravity. *Science Progress*, 1984, v. 69, no. 273, 1–17.
11. Kundan A. et al. Condensation on Highly Superheated Surfaces: Unstable Thin Films in a Wickless Heat Pipe. *Phys. Rev. Lett.*, 2017, v. 118, 094501.
12. Alshibli Kh. et al. Strain Localization in Sand: Plane Strain versus Triaxial Compression. *Journal of Geotechnical and Geoenvironmental Engineering*, 2003, v. 129, no. 6.

13. Alshibli Kh. Behavior of granular materials in microgravity environment: implication for future exploration missions. *Infrastruct. Solut.*, 2017, v. 2, 22.
14. Hoson T. Plant Growth and Morphogenesis under Different Gravity Conditions: Relevance to Plant Life in Space. *Life*, 2014, v. 4, 205–216.
15. Verlinde E. On the Origin of Gravity and the Laws of Newton. arXiv:1001.0785v1 [hep-th], (2010).
16. Bechinger C., Grünberg H., Leiderer P. Entropische Kräfte. *Physikalische Blätter*, 1999, v. 55, no. 12.
17. Nicolini P. Entropic force, noncommutative gravity and ungravity. arXiv:1005.2996v3 [gr-qc], (2010).
18. Kobakhidze A. Gravity is not an entropic force. arXiv:1009.5414v2 [hep-th], (2010).
19. Motloch L.N. Effects of Pre-Sowing Incubation within a Pyramid on Germination and Seedling Growth of Phaseolus Vulgaris L. // Master of Science Thesis, Tarleton State University, (2017).
20. Skliarov A. Biological Experiments in the Egyptian Pyramids. LAH, www.lah.ru, (2009).
21. Müller H. Quantum Gravity Aspects of Global Scaling and the Seismic Profile of the Earth. *Progress in Physics*, 2018, v. 14, 41–45.
22. Kosyrev N.A. Astronomical observations through the physical properties of time. // Kosyrev N. A. Selected Works. Leningrad, 363–383, (1991).
23. Müller H. Fractal Scaling Models of Natural Oscillations in Chain Systems and the Mass Distribution of Particles. *Progress in Physics*, 2010, v. 6, no. 3, 61–66.
24. Ries A. Qualitative Prediction of Isotope Abundances with the Bipolar Model of Oscillations in a Chain System. *Progress in Physics*, 2015, v. 11, 183–186.
25. Müller H. Scale-Invariant Models of Natural Oscillations in Chain Systems and their Cosmological Significance. *Progress in Physics*, 2017, vol. 13, 187–197.
26. Khintchine A.Ya. Continued fractions. University of Chicago Press, Chicago, (1964).
27. Hilbert D. Über die Transcendenz der Zahlen e und π. *Mathematische Annalen*, 1983, v. 43, 216–219.
28. Dombrowski K. Rational Numbers Distribution and Resonance. *Progress in Physics*, 2005, v. 1, no. 1, 65–67.
29. Panchelyuga V.A., Panchelyuga M. S. Resonance and Fractals on the Real Numbers Set. *Progress in Physics*, 2012, v. 8, no. 4, 48–53.
30. Müller H. The general theory of stability and objective evolutionary trends of technology. Applications of developmental and construction laws of technology in CAD. Volgograd, VPI, (1987).
31. Müller H. Superstability as a developmental law of technology. Technology laws and their Applications. Volgograd-Sofia, (1989).
32. Laplace P. Mechanique Celeste. pp. 642–645, (1825).
33. Van Flandern T. The Speed of Gravity — What the Experiments Say. *Physics Letters A*, 1998, v. 250, 1–11.
34. Müller H. Global Scaling. The Fundamentals of Interscalar Cosmology. *New Heritage Publishers*, Brooklyn, New York, USA, (2018).
35. Müller H. Emergence of Particle Masses in Fractal Scaling Models of Matter. *Progress in Physics*, 2012, v. 8, no. 4, 44–47.
36. Ries A. A Bipolar Model of Oscillations in a Chain System for Elementary Particle Masses. *Progress in Physics*, 2012, v. 8, no. 4, 20–28.
37. Ries A., Fook M. Fractal Structure of Nature's Preferred Masses: Application of the Model of Oscillations in a Chain System. *Progress in Physics*, 2010, v. 6, no. 4, 82–89.
38. Ries A. The Radial Electron Density in the Hydrogen Atom and the Model of Oscillations in a Chain System. *Progress in Physics*, 2012, v. 8, no. 3, 29–34.
39. Müller H. Fractal scaling models of natural oscillations in chain systems and the mass distribution of the celestial bodies in the Solar System. *Progress in Physics*, 2010, v. 6, no. 4, 44–47.
40. Müller H. Global Scaling as Heuristic Model for Search of Additional Planets in the Solar System. *Progress in Physics*, 2017, v. 13, 204–206.
41. Müller H. Chain Systems of Harmonic Quantum Oscillators as a Fractal Model of Matter and Global Scaling in Biophysics. *Progress in Physics*, 2017, v. 13, 231–233.
42. Müller H. Astrobiological Aspects of Global Scaling. *Progress in Physics*, 2018, v. 14, 3–6.
43. Müller H. Global Scaling of Planetary Systems. *Progress in Physics*, 2018, v. 14, 99–105.
44. Müller H. Global Scaling of Planetary Atmospheres. *Progress in Physics*, 2018, v. 14, 66–70.
45. Müller H. Gravity as Attractor Effect of Stability Nodes in Chain Systems of Harmonic Quantum Oscillators. *Progress in Physics*, 2018, v. 14, 19–23.
46. Staude J. Untersuchung granularer Materie am Beispiel des Laufzeitverhaltes einer Sanduhr unter Einwirkung äußerer Kräfte. Bachelor Thesis Physics, Freie Universität Berlin, (2013).
47. Olive K.A. et al. (Particle Data Group), Physical Constants. *Chin. Phys. C*, 2016, v. 38, 090001.
48. Beverloo W.A., Leniger H.A., van de Velde J. The flow of granular solids through orifices. *Chem. Eng. Sci.*, 1961, v. 15, 260–269.
49. Mankoc C. et al. The flow rate of granular materials through an orifice. arXiv:0707.4550v1 [cond-mat.soft], (2007).
50. Pavlov D.G. Chronometry of the Three-Dimensional Time. // Space-Time Structure. Algebra and Geometry. Russian Hypercomplex Society, Moscow, (2007).